LWT - Food Science and Technology 152 (2021) 112339

Contents lists available at ScienceDirect

LWT

journal homepage: www.elsevier.com/locate/lwt

Fourier-transform infrared (FTIR) fingerprinting for quality assessment of protein hydrolysates

Ingrid Måge *, Ulrike Böcker, Sileshi Gizachew Wubshet, Diana Lindberg, Nils Kristian Afseth

Nofima - Norwegian Institute of Food, Fisheries and Aquaculture Research, P.O. Box 210, N-1431, Ås, Norway

ARTICLE INFO

Keywords:
Enzymatic hydrolysis
Rest raw materials
FTIR fingerprinting
Data integration
Multivariate product optimisation

ABSTRACT

Enzymatic protein hydrolysis can be used industrially for refining peptides from poultry by-products. The aim is to introduce these peptides for human consumption, but today the majority is used for feed or pet food. One main barrier for entering the human market is unknown and unstable peptide product qualities. Reliable analytical methods for characterising the peptide fraction is therefore vital for optimizing and controlling the product quality.

In this work, we investigate the potential of using a large database of dry-film Fourier-transform Infrared (FTIR) fingerprints to gain new insight in quality variations of peptide products. The database cover >1300 samples from laboratory experiments performed over several years. We found that the FTIR fingerprints contain patterns that are stable across experiments and time, and that variations in the fingerprint can be related to raw material composition and processing factors.

We also show that the database can be used for evaluating industrial samples. By comparing the FTIR fingerprints of industrial samples with those in the database, we could see systematic changes in product quality over time and make hypotheses about the underlying causes for change. These results lay the foundation for using dry-film FTIR spectroscopy as an industrial tool for product and process optimisation and control.

1. Introduction

Sustainable utilisation of raw materials and the urgent need for more and better proteins for human consumption has led the food industry to invest heavily in bioprocesses that can transform by-products into nutritionally valuable proteins. One such process is enzymatic protein hydrolysis (EPH), where enzymes break down proteins into smaller peptides and amino acids. This technology is widely used in production of e.g. sports nutrition and infant formulations from diary by-products (Nasirpour, Scher, & Desobry, 2006; Tang, Moore, Kujbida, Tarnopolsky, & Phillips, 2009), and it is increasingly used in the meat and fish industry for refining peptides from poultry and fish by-products (Aspevik et al., 2017). The industry aims at introducing peptides from fish and poultry as nutritional supplements or ingredients for human consumption, but today the majority is used for feed or pet food.

By-products from poultry and fish mainly consist of skin, bones, muscle residues, adipose tissue, and connective tissue. When processing with EPH, the raw materials are ground and mixed with water and enzymes. After 30–60 min reaction time at around 50 °C, three crude fractions are recovered: a peptide-rich liquid fraction, a lipid-rich fraction, and a mineral-rich sediment. Whereas the lipid fractions from fish by-products have found high-paying human markets, the peptide fractions are currently only to a small degree turned into high-value products for human consumption. One main barrier for entering the human market is the large variation in peptide size distribution. This peptide population largely defines the product quality and thus the market opportunities. Unlike dairy by-products, the by-products from poultry and fish are inhomogeneous and have substantial variation in composition. This leads to a complex and variable composition of the hydrolysate. Reproducible and reliable analytical methods for characterisation of the peptide fraction, during and after processing, is therefore vital for entering the human market.

Several potential sensors for monitoring EPH processes have been proposed. Near-Infrared (NIR) spectroscopy is a flexible process-monitoring tool frequently used in the food industry (Grassi & Alamprese, 2018; Porep, Kammerer, & Carle, 2015). The technique is first and foremost employed for quantification of gross composition of foods, and NIR cannot necessarily provide detailed information on

* Corresponding author.
E-mail address: ingrid.mage@nofima.no (I. Måge).

https://doi.org/10.1016/j.lwt.2021.112339
Received 18 March 2021; Received in revised form 19 August 2021; Accepted 19 August 2021
Available online 21 August 2021

protein structural changes required in EPH processes (Garrido-Varo, Vega, Maroto-Molina, De La Haba, & Pérez-Marín, 2016). Recently, low-field nuclear magnetic resonance (NMR) spectroscopy was used for real-time monitoring of EPH of marine by-products (Anderssen & McCarney, 2020). The approach was used for prediction of reaction rates, but further investigations on the ability to detect changes in protein chain lengths are still needed.

Fourier-transform Infrared spectroscopy (FTIR) presents opportunities to characterise hydrolysate products at critical control points in production lines. FTIR is a vibrational spectroscopy technique that can be used to measure molecular structures and the composition of molecular mixtures. The FTIR spectrum of a biological sample is commonly denoted a fingerprint, as it provides a unique spectral signature of the sample. Poulsen et al. (2016) demonstrated the use of liquid FTIR measurements to estimate degree of hydrolysis, i.e. the extent to which proteins are broken down into protein fragments and peptides, during EPH of whey proteins. The approach was promising, but in liquid FTIR analysis, important protein-related features in the spectra are lost due to water absorption. Thus, dry-film FTIR spectroscopy has been introduced to follow the breakdown of proteins both qualitatively and quantitatively by predicting average molecular weights of protein hydrolysates (Böcker, Wubshet, Lindberg, & Afseth, 2017; Kristoffersen et al., 2019, 2020; Wubshet et al., 2017). Average molecular weights are generally correlated to the degree of hydrolysis (Kristoffersen et al., 2020). Moreover, molecular weight distributions that can be derived from FTIR spectra are related to industrially relevant quality parameters such as bioactivity, sensory attributes, and functional properties (García Arteaga, Apéstegui Guardia, Muranyi, Eisner, & Schweiggert-Weisz, 2020; Li et al., 2013). Therefore, it is expected that FTIR can provide an analytical platform for real time control of these characteristics in the future.

In addition to end-product quality control, monitoring of product quality can be used in process and product optimisation, inspired by the Quality by Design (QdB) and Process Analytical Technology (PAT) initiative that is widely acknowledged in pharmaceutical industry (FDA, 2004). Knowledge about the relationships between raw material composition, processing parameters and end-product quality can enable the industry to steer the production towards specific targets, either by designing processes that are robust towards known variations (QdB) or by continuously measuring raw material composition and adjusting the process in a feed-forward manner (Wubshet et al., 2018).

The common way of using FTIR in process monitoring is to build calibration models for preferred product qualities (e.g. protein and fat contents of milk, or average molecular weights of protein hydrolysates). In other applications, like for instance food authenticity, the FTIR fingerprint is used directly to build classification models to sort samples into “authentic” or “adulterated” (Hassoun et al., 2020; Valand, Tanna, Lawson, & Bengtström, 2020). Similar approaches are currently used in genetics, where the FTIR fingerprints are used directly as phenotypes and are linked to heritability parameters (Wang, Hulzebosch, & Bovenhuis, 2016; Zaalberg, Shetty, Janss, & Buitenhuis, 2019). The concept of using spectral fingerprints directly for process monitoring and optimisation (without building calibration models for specific chemical parameters) is not new, but the majority of such publications consider fermentation processes, and industrial scale case studies are few (Gargalo et al., 2020). In this work, we will investigate the potential of using a large database of dry-film FTIR fingerprints from a collection of laboratory experiments to gain new insight in quality variations of EPH products. Specifically, we will investigate the effects of raw material composition and process parameters on the fingerprints. Moreover, we will assess whether the database can be used for benchmarking of industry samples.

2. Materials and methods

We have gathered data from six laboratory experiments conducted in the time interval 2014–2019. All the experiments involved enzymatic hydrolysis of by-products from poultry, but the aims and experimental designs differed. For all experiments, the enzyme type and hydrolysis time is known, and the hydrolysates were characterized by dry-film FTIR spectroscopy. For a subset of the experiments, proximate analyses of the raw materials are also available.

We also gathered samples from one newly established large-scale industry plant, and three comparable products from a different commercial actor. The industry samples were collected in three separate periods: spring 2019, autumn 2019 and autumn 2020. The enzyme type is known for the industrial plant, but the raw material composition and exact hydrolysis time is unknown. An overview of the laboratory experiments and industrial sampling series is given in Table 1.

2.1. Raw materials

The industry-scale plant receives fresh by-products directly from a Norwegian poultry slaughterhouse. The raw material composition varies substantially from day to day depending on the production of main poultry products. For the laboratory-scale hydrolyses, raw poultry materials were collected from the same slaughterhouse. On the day of collection, samples were ground using a Seydelmann SE130 meat grinder (Seydelmann, Stuttgart, Germany), mesh size of 0.5 or 1 cm. After grinding, the minced raw materials are aliquoted, flat-packed, and vacuumed before stored frozen at either −20 °C or −40 °C until the day of hydrolysis.

2.2. Laboratory scale enzymatic protein hydrolysis

The laboratory scale hydrolysis experiments were performed as batch processes. The frozen minced raw materials were thawed at room temperature and mixed in a 1:2 ratio (raw material:water) in a Reactor-Ready™ jacketed reaction vessel (Radleys, Saffron Walden, Essex, United Kingdom). The mixture was heated during stirring and kept at the correct temperature (50 °C) during the enzymatic reaction. At t = 0, the appropriate amount of enzyme (0.5–1%, w/w) was added and the reaction was run for a defined time. The enzymatic reaction was terminated using first fast microwave heating in a Menumaster commercial microwave oven (ACP, IA, USA), where after the temperature was kept at a minimum of 90 °C for 15 min in a heated water bath. Samples were centrifuged (15 min, 4400 rpm, 25 °C), the sediment was removed and lastly, water and fat-phase were separated using a separator funnel. The water phase was aliquoted and stored frozen at −40 °C until lyophilized (CHRIST 1–16 LSCplus, Germany). Samples taken during hydrolysis (before batch completion) were heat inactivated as described above and filtered through a Millex-HV PVDF 0.45 μm 33 mm filter (MilliporeSigma, Billerica, MA, USA) before stored frozen (−20 °C) in Falcon tubes until measurements.

2.3. Industry scale enzymatic protein hydrolysis

Unlike the laboratory experiments, the industrial EPH is a continuous flow process. The commercial enzyme used in this process is subsequently referred to as “industry enzyme”. The hydrolysates obtained from this process were sampled manually after heat inactivation (i.e. termination of the enzymatic reaction) but before phase separation. All samples were stored frozen and brought to the laboratory for phase separation (as described in section 2.2.) prior to measurements.

The three samples from the other commercial actor were received as hydrolysate powders, and nothing is known about the production of these except that they are based on poultry raw materials.

2.4. FTIR measurements

Samples from laboratory and industry were all measured in the same way using the same FTIR instrument. Eight μL liquid hydrolysate

Table 1
Overview of data sources.

Data source	Raw materials	Enzymes	Number of independent hydrolysis runs	Number of hydrolysate samples	Raw material composition available
LAB1[a]	Chicken/Turkey	Alcalase 2.4L	30	30	YES
LAB2[b]	Chicken/Turkey	Alcalase 2.4L	12	129	Partly
LAB3[c]	Chicken/Turkey	Alcalase, Papain, Protamex	27	324	Partly
LAB[d]	Chicken/Turkey	Alcalase 2.4L, Corolase 2 TS, Flavourzyme	59	705	YES
LAB5[e]	Chicken	Alcalase 2.4L, Flavourzyme, "Industry enzyme" +13 other enzymes	29	105	NO
LAB6[e]	Chicken	Alcalase 2.4L, Corolase 2 TS, Flavourzyme	17	95	YES
IND1[f]	Chicken/Turkey	"Industry enzyme"	5	5	NO
IND2[g]	Chicken/Turkey	"Industry enzyme"	46	46	NO
IND3[h]	Chicken/Turkey	"Industry enzyme"	105	105	NO
COMP[i]	Chicken/Turkey	Unknown	3	3	NO

[a](Wubshet et al., 2018), [b](Wubshet et al., 2017), [c](Kristoffersen et al., 2019), [d](Kristoffersen, 2019), [e]Unpublished, [f]Spring 2019, [g]Autumn 2019, [h]Autumn 2020, [i]Another commercial actor.

samples (either directly sampled from water phase or reconstituted from hydrolysate powder) were transferred onto 96-well IR-transparent Si-plates and left to dry for at least 45 min to form dry hydrolysate films. From all the samples, a total of five replicate FTIR dry-films were prepared to account for possible variations in the liquids. All FTIR measurements were performed with a High-Throughput-Screening-Extension (HTS-XT) coupled to a Tensor 27 spectrometer (Bruker Optics, Germany). Acquisition of transmission spectra was controlled by OPUS v6.5 software. All spectra were collected in a range from 4000 to 400 cm^{-1} with a resolution of 4 cm^{-1}, an aperture of 5.0 mm and a total of 40 scans. Prior to each sample measurement, background spectra (same number of scans as the sample spectra) of the Silicon plate were obtained to account for variation in water vapour and CO_2.

All raw spectra were subjected to a quality test (QT) examining absorbance intensity, signal-to-noise ratio and water vapour content (Lovergne et al., 2015; Zhang et al., 2013). The QT parameters are derived from the parameters suggested in the OPUS v6.5 software (Bruker Optics, Germany). Absorbance was evaluated in the region 2100-1600 cm^{-1}, and spectra with a absorbance range higher than 1.5 or lower than 0.1 were excluded. Signal-to-noise ratio was calculated from first derivative spectra, taking the signal range of the Amide I band between 1700 and 1600 cm^{-1} (S1) and between 1200 and 960 cm^{-1} (S2) respectively divided by the noise range evaluated between 2100 and 2000 cm^{-1} (N). Spectra were rejected when S1/N was less than 50 and S2/N was less than 10. Water vapour content (W) was evaluated between the 1847–1837 cm^{-1}. Spectra were rejected when S1/W was less than 20 and S2/W was less than 4.

A second derivative was applied to the spectra using the Savitzky-Golay algorithm with a polynomial degree of two and a smoothing window size of 13 points. Additionally, all spectra were normalized using standard normal variate (SNV). Then, spectra from replicate hydrolysate dry-films were averaged to provide one single spectrum per sample, and the region between 1700 and 800 cm^{-1} was used for further analysis.

2.5. Data analysis

The novel correlation coefficient ϕ_K is used to evaluate confoundings in metadata (Baak, Koopman, Snoek, & Klous, 2020). This is a generalisation of the Pearson correlation coefficient that can be used for categorical, ordinal and continuous variables. It is therefore well suited to assess confoundings between metadata of different types, in this case between categorical factors such as enzyme type and experiment and continuous variables representing hydrolysis time and raw material composition.

Principal component analysis (PCA) is used to transform the FTIR spectra linearly to a lower dimensional space. The advantage of PCA is that it decomposes the variation into orthogonal components, and it is straight forward to project new samples onto the subspace. The loadings can be used to interpret the main sources of variation spanning each of the components, but the components are not necessarily expected to represent specific properties or chemical components. In this paper we refer to this model as *FTIR-PCA*, and scatter plots of scores as the *FTIR-PCA map*.

Sequential Orthogonalized PLS regression (SO-PLS) is used to relate the FTIR-PCA scores to raw material and processing variables (Næs, Tomic, Afseth, Segtnan, & Måge, 2013). This method introduces blocks of variables sequentially, which enables quantification and interpretation of the individual block contributions. In this context we split the data in 1) raw material quality, 2) process settings (see definitions below). Interactions between raw material quality and process settings are included as a third block, as described in (Næs, Måge, & Segtnan, 2011). In matrix notation, the model for predicting scores from FTIR-PCA component i can be written as:

$$\mathbf{FTIRscore}_i = \mathbf{X}_{RM}\mathbf{b}_{i,RM} + \mathbf{X}_P\mathbf{b}_{i,P} + \mathbf{X}_{RM\ x\ P}\mathbf{b}_{i,RM\ x\ P} + \mathbf{f}_i$$

where *RM* and *P* stand for "Raw Material" and "Processing" respectively, **X** are matrices of predictor variables, **b** are regression coefficient vectors and **f** are residuals. The $\mathbf{X}_{RM}$ block contains variables *Fat%*, *Protein%*, *Ash%*, their interactions, squared effects, and pairwise ratios, as well as the *Chicken/Turkey* proportion, in total 13 variables. The $\mathbf{X}_P$ block includes linear and squared *Hydrolysis time*, 0/1 dummy variables for *Enzymes*, and interactions between enzymes and time variables, in total 11 variables. The interaction block $\mathbf{X}_{RM\ x\ P}$ contains 154 variables, representing all interactions between variables in the first two blocks. The models were validated by segmented cross-validation, where all samples from the same hydrolysis run is held out in each segment. Optimal number of components were selected by the global approach, where all combinations of components (up to a maximum) are evaluated, as described in e.g. (Næs et al., 2013)

Systematic differences between experiments were evaluated both *within* and *outside* the FTIR-PCA subspace. For the *outside* part, sample residuals after nine FTIR-PCs were analysed by 1-way ANOVA. For the *within* part, Soft Independent Modelling of Class Analogies (SIMCA) (Wold & Sjöström, 1977, pp. 243–282) was performed on the combined cross-validated Y-residuals from nine SO-PLS models, to see if there were

experiment-specific patterns in the FTIR-PCA space that were not modelled by the explanatory variables. SIMCA is a supervised classification technique that allows samples to belong to more than one class. It is therefore well suited to evaluate overlap between classes, which is especially interesting in this context as we want to investigate if the experiments are overlapping. The classification model was assessed by the proportion of samples classified into multiple classes, as well as the class-specific *sensitivity* and *specificity* values. *Sensitivity* is calculated as number of true positives divided by total number of samples in each class, i.e. the fraction of the class that is correctly classified. *Specificity* is calculated as the number of true negatives divided by the total number of samples *not* belonging to a given class, i.e. the fraction of samples in other classes that are correctly identified to be outside the given class.

3. Results

The results are divided in four subsections. The first three investigate the potential of using the database for gaining new insights by 1) explorative analysis of the FTIR fingerprints and metadata, 2) predicting FTIR fingerprint from metadata, and 3) assessing systematic differences between experiments. The fourth subsection shows how the database can be used for benchmarking industry samples.

3.1. Explorative analysis of the database

All the spectra were merged in a common data structure, with the following metadata connected to each hydrolysate sample:

- Experiment (or sampling period for industry samples)
- Hydrolysis run (or batch ID)
- Raw material composition (fat, protein and ash percentages)
- Type of enzyme
- Hydrolysis time
- Production scale (lab or industry)

The experiments were designed for different research questions, which leads to confoundings and dependencies among the metadata. This is important to consider when interpreting relations between metadata and the spectra. The ϕ_K correlations between metadata are illustrated in Fig. 1. We see that Experiment and Enzyme are highly correlated (=0.83) for the full sample set (Fig. 1A). This is because some enzymes were only used in one or a few of the experiments, especially in the LAB5 experiment where 16 different enzymes were screened. Hydrolysis time, however, has low correlation with both Enzyme and Experiment, which means that effects of hydrolysis time can be estimated independently of both Experiment and Enzyme.

A principal component analysis was performed on 1324 hydrolysates from the lab experiments. Samples from pure muscle and mechanically deboned meat of less than 10 min hydrolysis time were removed because they were outlying in some of the components and not deemed to be industrially relevant. The first two components explain the majority of the spectral variation (72%), but as many as nine components were found to have structured variation that could be related to raw material quality or processing (further described in section 3.2). Scores of FTIR-PCA components are given in Fig. 2 (as scatter plots) and Fig. 3 (enzyme-averages as function of hydrolysis time). The corresponding loadings are given in Fig. 4. Here, the average FTIR spectrum of all hydrolysates are provided for comparison, and annotations of important FTIR bands are provided in Table 2.

PC1 and PC2 show a clear time effect at the same time as it separates Flavourzyme from the other enzymes. This separation is expected, since Flavourzyme is a pure exopeptidase and cleaves the terminal peptide bonds of the proteins. The result is amino acids and small peptides and thus a completely different peptide composition compared to most of the other enzymes in the study (endopeptidases cleaving in the middle of the proteins). The loading plots for PC1 and PC2 (Fig. 4) confirm this, and the most important bands related to Flavourzyme are the symmetric and asymmetric stretching of COO^- (region *iii* and *vii* in Fig. 4 and Table 2), and the NH_3^+ deformation (region *v)* (Böcker et al., 2017; Kristoffersen et al., 2020). They will all increase with the formation of C-terminals (COO^-) and N-terminals ($NH3^+$) in the arising peptides and the release of free amino acids. Protamex is separated from the other enzymes in several of the minor components (PC3, PC4, PC7 and PC8), while differences between Papain and Corolase span the variation in PC9. Based on the loadings shown in Fig. 4, these components are mainly related to changes in the amide I region (*i* and *ii*) as well as region *viii* and *ix*. The variations are most likely related to the different affinities of the enzymes for different proteins present in the poultry by-products used (e.g. connective tissue vs. myofibrillar proteins) (Kristoffersen et al., 2019). From Fig. 3 we also see that the time trajectories vary substantially between enzymes in many of the FTIR-components, indicating differences in reaction kinetics.

3.2. Effect of raw materials and processing on FTIR fingerprint

A subset of the full sample set, for which raw material composition is known, is used to relate enzyme, processing time and raw material composition to the FTIR-PCA components. This subset contains 908 hydrolysates, from 114 independent hydrolysis runs and 22 different raw material batches. It covers three different enzymes (Alcalase,

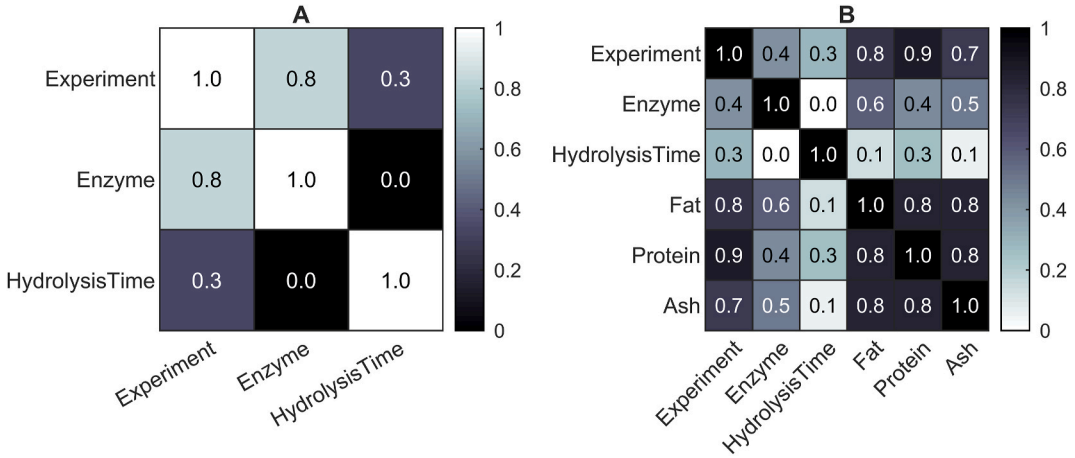

Fig. 1. Correlations between metadata, based on (A) the 1324 samples used to create the FTIR-PCA model. (B) The subset of 908 samples for which the raw material composition is known.

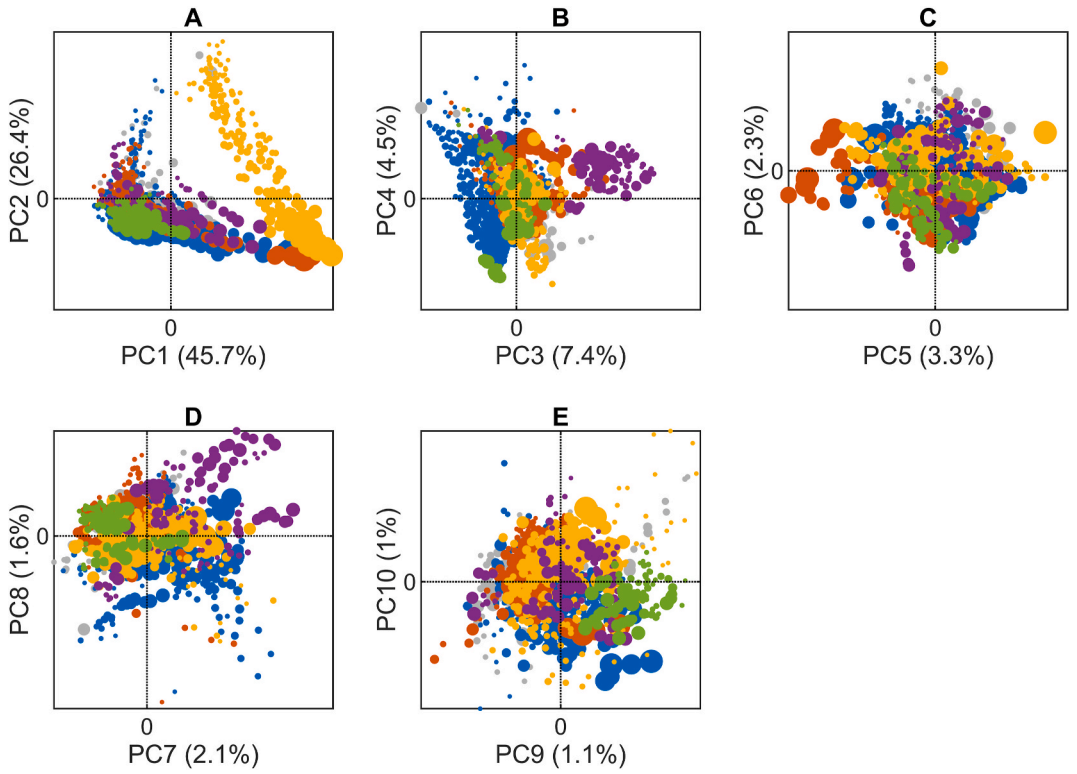

Fig. 2. Scores for the first ten FTIR-PCA components. The dot size is proportional to hydrolysis time, and colour represent different enzymes (blue = Alcalase, red = Corolase, yellow = Flavourzyme, purple = Protamex, green = Papain). Enzymes with less than 80 samples (all from Experiment "LAB5") are all coloured light grey. (For interpretation of the references to colour in this figure legend, the reader is referred to the Web version of this article.)

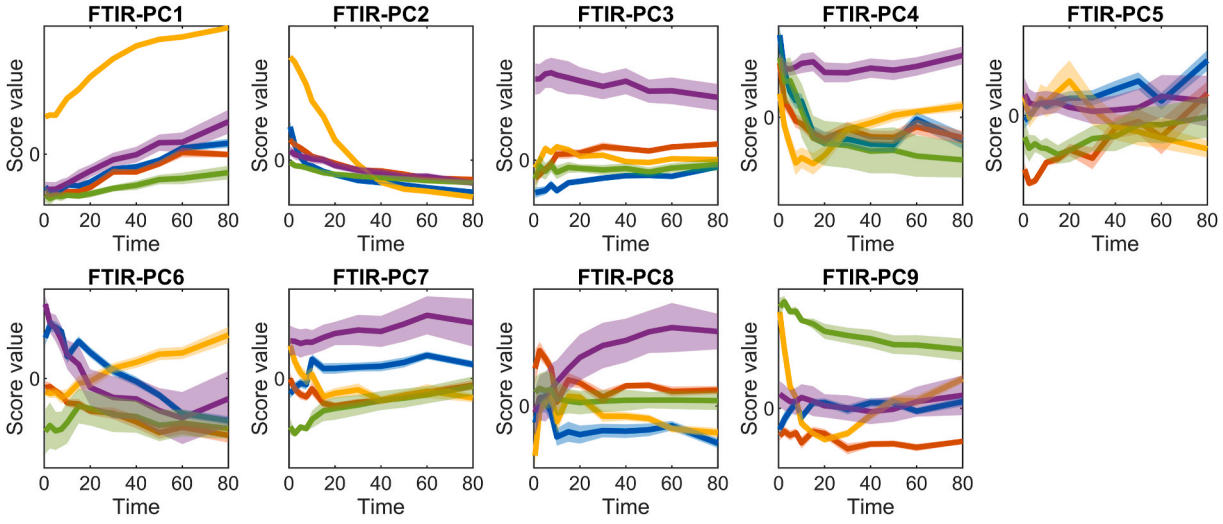

Fig. 3. Average score time trajectories for each FTIR-PCA component and enzyme (blue = Alcalase, red = Corolase, yellow = Flavourzyme, purple = Protamex, green = Papain). The shaded area represents ± standard error of the mean. Enzymes with less than 80 samples (from Experiment "LAB5") are not included in the figure. (For interpretation of the references to colour in this figure legend, the reader is referred to the Web version of this article.)

Corolase and Flavourzyme), and spans hydrolysis times from 0.5 to 80 min.

The correlation between metadata for this subset is shown in Fig. 1B. We see that the correlation between Enzyme and Experiment is much lower (=0.41) than for the full data set, meaning that this subset is better suited for estimating enzyme effects across experiments. The raw material components protein, fat and ash are however highly correlated, which is expected for compositional variables. These are also correlated to experiment, which means that the raw material composition varies systematically between experiments. This is mainly because two of the experiments use pure chicken muscle, which is much higher in protein and lower in fat than the by-products. Inference about individual raw material components can therefore not be made, but effects of changes in overall composition can still be modelled.

SO-PLS regression was used to evaluate contributions from the three blocks of variables representing raw material quality (RM), processing (P), and interaction between raw material quality and processing (RM x P). Models were fitted to the first twenty FTIR-PCA components, and valid models were obtained for the first nine components, see Table 3. These nine components explain 94.4% of the variation in FTIR

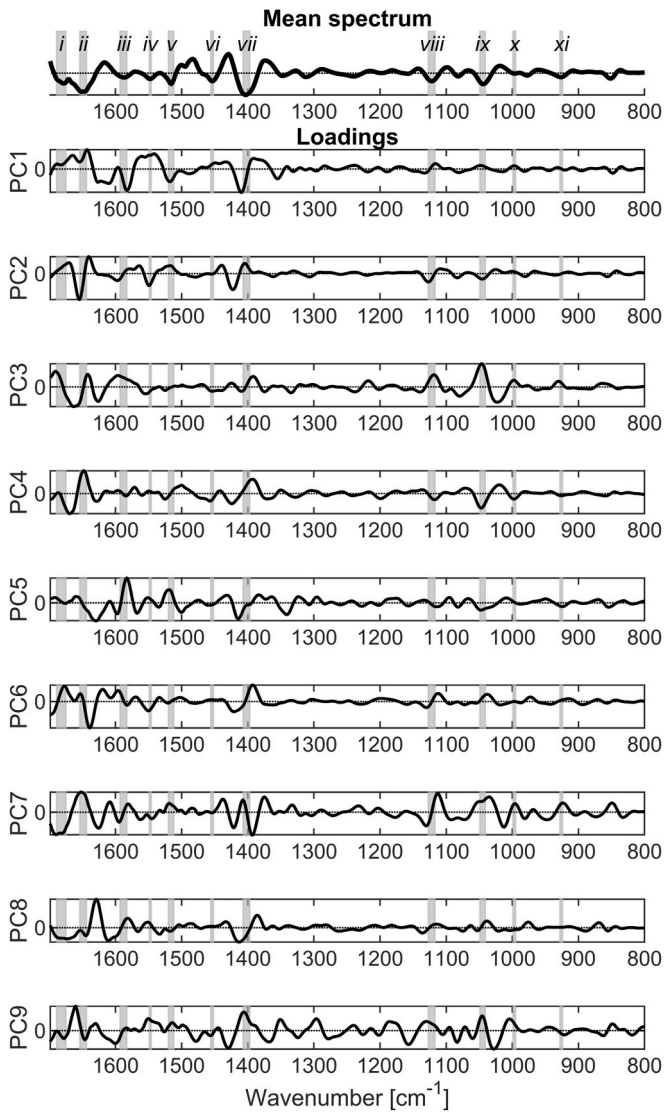

Fig. 4. Average 2nd derivative spectrum (top) and loadings for the first nine FTIR-PCA components, corresponding to the scores Fig. 2 and 3. The most important bands are highlighted, with annotations given in Table 2.

Table 2
Annotation of the most important 2nd derivative FTIR bands, corresponding to spectra and loadings in Fig. 4.

	Annotation	Region, cm^{-1}
i	C=O turns (amide I)	1689–1675
ii	C=O α-helix (amide I)	1654–1644
iii	COO^- *asym* stretch (amide II)	1593–1583
iv	α-helix (amide II)	1549–1546
v	$-NH_3^+$ scissor	1520–1512
vi	CH_2 scissor	1456–1452
vii	COO^- *sym* stretch	1407–1397
viii	CNH_3 rock, CH_2 wag	1127–1117
ix	CO, CC, CN stretch	1049–1041
x	CCOO wagging	999–995
xi	CH_2 twist	928–924

fingerprints, and 77% can be modelled by the explanatory variables (cross-validated). Recall that the first two components accounted for 72% of the variation in the FTIR-PCA, and these are also best predicted, with cross-validated explained variances ≈90%. The process settings (i.e. enzyme type and hydrolysis time) are clearly the most important for predicting FTIR-PC1 and FTIR-PC2, as already inferred from Figs. 2A and 3. We also know from Fig. 3 that PC3, FTIR-PC4, FTIR-PC7, FTIR-PC8 and FTIR-PC9 mainly span variation caused by Protamex and Papain. These enzymes are not included in the subset used for regression, and we did not expect to be able to model these components well. Even so, the validated explained variances are between 53 and 58%, with contribution coming from both raw material and the process variables. Closer inspection of the model parameters reveals that FTIR-PC3 represents variation specific to Alcalase, while FTIR-PC9 represents differences in time effects between Flavourzyme and the other enzymes.

Note that FTIR-PC4, FTIR-PC7 and FTIR-PC8 have substantial contributions (>36%) from the raw material composition. The compositional nature of raw material variables *Protein*, *Fat* and *Ash* means that their effects cannot be interpreted independently. The effect of these three constituents is therefore visualised in a two-dimensional subspace, explaining 86% of the variation in protein, fat and ash (Fig. 5). We see that the steepest ascent in FTIR-PC4 is in the direction of increasing fat content (i.e. decreasing protein), while increasing ash content represents the steepest descent/ascent in FTIR-PC7/FTIR-PC8.

FTIR-PC5, FTIR-PC6 and FTIR-PC9 have substantial contributions from the interaction block. This means that different raw material qualities need different processing to obtain the same FTIR fingerprint. This is especially interesting regarding process control and optimisation, indicating that the process should be adjusted based on the raw material composition in order to obtain stable end-product quality. Interpretation of these interaction effects is not straightforward but can for instance be done by constructing a range of raw material contour plots for different enzymes and hydrolysis times (not shown).

3.3. Evaluating systematic differences between experiments

The squared sample residuals after nine FTIR-PCA components were compared in a one-way ANOVA. Results showed that there were systematic differences between experiments ($p < 0.001$). The distributions of residuals are plotted in Fig. 6A. Specifically, LAB1, LAB5 and LAB6 have significantly higher residuals than the other experiments. Even so, the distributions are highly overlapping and does not reveal any severe problems. The experiments were performed by different scientists and laboratory technicians, which could lead to variations in sampling and measurement errors and explain these observed differences.

SIMCA classification was performed on the combined cross-validated Y-residuals from the nine SO-PLS models. Results showed that only 5% of the samples were assigned to one single experiment, while 11%, 64% and 20% were assigned to two, three and four experiments, respectively. This shows that there is a high degree of overlap between experiments. The sensitivity and specificity for each experiment is given in Table 4. The sensitivity is high in all cases, but only *LAB2* and *LAB3* have a high specificity, meaning that these experiments have a smaller overlap than the other experiments. We know that *LAB2* and *LAB3* are different from the others because they contain hydrolysates of pure chicken fillet. It is therefore not surprising that the spectra contain information that discriminates them from the experiments that are based on by-products only.

3.4. Benchmarking of industry-scale products

Four sets of industry samples (described in Table 1) were projected onto the FTIR-PCA map, to evaluate if the lab hydrolysates are representative for industry products and to assess the variation in product qualities (Fig. 7). IND1, IND2 and IND3 were sampled from a newly established EPH plant during spring 2019, autumn 2019 and autumn 2020, respectively. COMP are products from a different commercial actor. Laboratory samples from the same enzyme as used in the industry plant are also highlighted in the map, for comparison.

There are clear systematic differences between all sample sets. Firstly, the industrial sampling series tend to move closer to the

Table 3
Summary of SO-PLS prediction models for the nine first FTIR-PCA components. The predictions are based on three blocks of explanatory variables, representing raw material compositions (RM), processing parameters (P) and interactions between the two (RM x P). The Root Mean Squared Error (RMSE) is normalized by range to make it comparable between models.

Response	Explained variance in FTIR-PCA (%)	# model components			Block-wise explained variance[a] (%)			Total explained variance [a] (%)	RMSE[a]	R^2
		RM	P	RM x P	RM	P	RM x P			
FTIR-PC1	45.7	0	2	1	0	89	5	94	0.06	0.94
FTIR-PC2	26.4	0	2	1	0	80	4	84	0.09	0.85
FTIR-PC3	7.4	2	2	0	9	44	0	53	0.10	0.54
FTIR-PC4	4.5	2	1	1	37	7	9	53	0.11	0.58
FTIR-PC5	3.3	2	1	3	14	12	19	45	0.11	0.57
FTIR-PC6	2.3	2	1	3	22	21	20	63	0.12	0.72
FTIR-PC7	2.1	2	0	2	43	0	13	56	0.09	0.61
FTIR-PC8[b]	1.6	1	0	3	36	0	19	55	0.09	0.59
FTIR-PC9	1.1	3	1	3	12	25	21	58	0.08	0.63
Total, all PCs	94.4							77		0.78

[a] Cross-validated.
[b] 36 outlying samples, with low scores in FTIR-PC8, were removed before modelling.

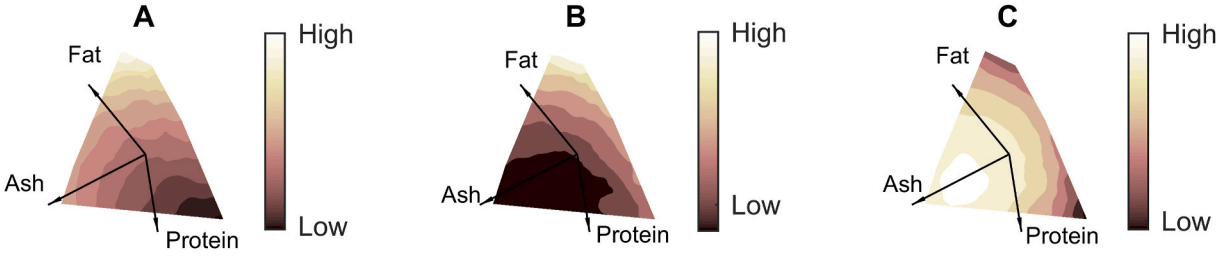

Fig. 5. Partial effect of raw material composition from the SO-PLS models predicting A) FTIR-PC4; B) FTIR-PC7; and C) FTIR-PC8. The contents of protein, fat and ash in raw materials are not independent, and contour plots are therefore shown as functions of two-dimensional subspace. The centre point represents average raw material composition, with arrows pointing towards increasing levels of fat, ash and protein. The contours are only shown for the area that is supported by data.

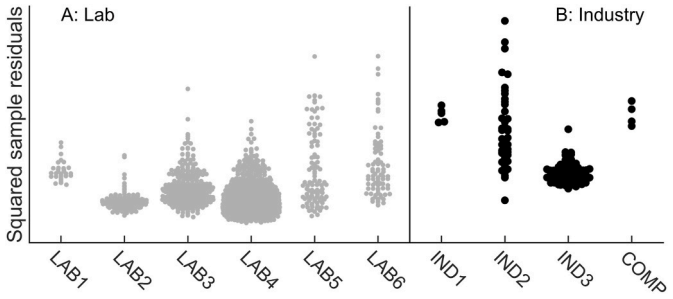

Fig. 6. Distribution of sample residuals from the FTIR-PCA model grouped by experiment (A) and industry site/period (B).

Table 4
Results for SIMCA classification of SO-PLS residuals. Note that LAB5 was not represented in the subset used for SO-PLS modelling and is therefore absent from the table.

	LAB1	LAB2	LAB3	LAB4	LAB6
Sensitivity	1.00	0.97	0.96	0.94	0.96
Specificity	0.07	0.98	0.88	0.47	0.03

comparable lab samples over time, and the variation within IND3 is considerably smaller than IND2. This suggests that the process is both closer to target and more stable in autumn 2020 compared to 2019, which agrees with the fact that the plant and the process was being established in the time period.

The spread is still relatively high in PC1 for the IND3 samples. PC1 explains most of the spectral variation and was therefore expected to be more stable. The spread of the samples from the other commercial actor (COMP) is however also large in this component.

The COMP samples are quite close to the IND3 samples in PC1-6 but differs in PC7-8. We know from the regression models that the first PCs mainly vary as a function of enzyme and time, while PC7-8 show variation caused by raw material composition. Based on this, we may hypothesise that the other commercial actor uses similar enzyme and hydrolysis time, while raw material might be different.

The sample residuals after nine FTIR-PCA components are shown in Fig. 5B. The residuals are somewhat higher for the industry samples compared to the lab samples, which is to be expected since the lab samples were used to fit the model and industry samples are likely to have components not present in the lab samples. Here too, we see that IND3 has considerably smaller residuals than the other industry sets, which points to the same conclusion as above: the products are more similar to lab samples and more stable during the IND3 sampling period. This shows that the lab samples are highly representative for the industrial products.

4. Discussion

A large part (77% in total) of the variation in FTIR fingerprints can be predicted from just a few, crude raw material and processing variables. Most of the variation is caused by differences in enzyme and hydrolysis time, but raw material composition is also contributing to several of the less dominant principal components. Although 77% is already a high number, the predictions are expected to improve if more relevant explanatory variables are included. For instance, process variables such as enzyme concentration, pH and temperature are known to affect the degree of hydrolysis, and the effects differ between enzyme types (Teshnizi, Robatjazi, & Mosaabadi, 2020; Sileshi G. Wubshet et al., 2019). Also, it is known from previous studies that the FTIR spectrum is sensitive to compositional changes in the protein hydrolysates due to raw material variations. This is obviously the case for raw materials of completely different origins, e.g. marine versus animal. But also changes

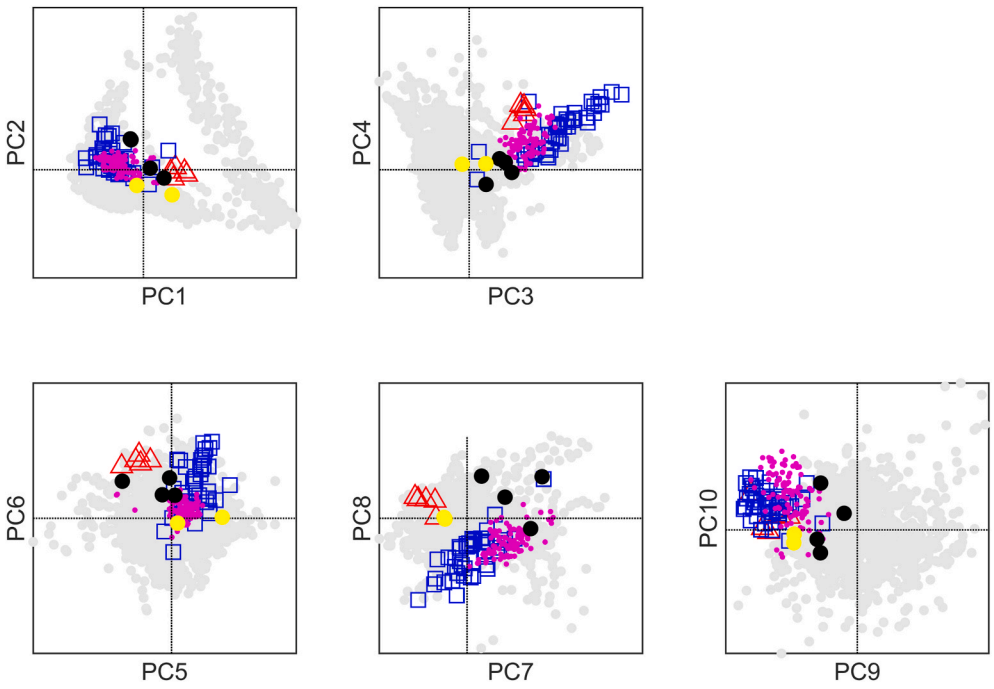

Fig. 7. Industry samples projected onto the FTIR-PCA map. The score plots are the same as in Fig. 2, with all the lab samples coloured light grey. Industry samples from EPH plant were collected in three periods as described in Table 1 (IND1 = red triangles, IND2 = blue squares, IND3 = small pink dots). Black dots represent products from a different commercial actor (COMP in Table 1), and yellow dots represent lab samples with the same enzyme and hydrolysis time as used in the plant. (For interpretation of the references to colour in this figure legend, the reader is referred to the Web version of this article.)

in the protein composition of the raw materials (e.g. connective tissue versus muscle proteins) can be seen in the corresponding FTIR spectra (Kristoffersen et al., 2019).

The type of prediction models developed in this study can for example be used for process monitoring and optimisation, especially if more parameters are included in the models as discussed in the previous section. Process monitoring can be performed using traditional multivariate statistical monitoring methods (Kourti, 2005). In such approaches, a target fingerprint is defined, for instance by defining a target area in the FTIR-PCA based on some gold standard product samples. If a deviation from the target area is detected for one or more FTIR-PCA components, the contributions of raw material and process parameters to these components can be used to diagnose the cause for deviation in retrospect. Alternatively, if raw material composition can be measured prior to processing, a feed-forward approach can be implemented (Sileshi Gizachew Wubshet et al., 2018). Relevant methods include prediction sorting (Berget & Næs, 2002) and model inversion (Vidal-Puig, Vitale, & Ferrer, 2019). The explanatory variables used in this work are however collected from lab processes and are not necessarily transferable to industry-scale production. For instance, preliminary investigations indicate that the hydrolysis time is not directly comparable between the lab-scale batch process and the industrial-scale continuous process. It is also not known how precise a model must be to be useful for the industry. More research is needed to model these relationships in industry scale, in order to develop robust and reliable feed-forward process control strategies.

The FTIR-PCA map presented in this paper spans a wide variation in raw materials and processing, probably much wider than what is seen in the industry. This is particularly the case for enzymes, which were shown to span a large part of the variation in several FTIR-PCA components (Figs. 2 and 3). Fig. 7 confirms that the industry samples only cover a fraction of the lab samples. For an industrial manufacturing company, it could be more beneficial to make a similar map based on their own samples only, which would give a more detailed representation of the relevant variation.

Some of the FTIR-PCA components explain very little of the spectral variation, for instance component 6–9 all explain <3%. These can still be relevant for the hydrolysate quality. A low explained variance may for example occur if the underlying chemical feature produce weak FTIR signals, which does not necessarily mean that it is unimportant. We would however expect that the uncertainty in these components is higher than the ones with higher explained variance.

Even if the combined data set has many samples (>900), the number of independent hydrolysis runs (= 114) and raw material batches (= 22) are low. There are also relatively high correlations between some of the explanatory variables and metadata (Fig. 1), which makes it hard to make inferences about causal relationships. We need to collect more data, preferably with known raw material composition, to validate the findings further.

Even if several molecular features are reflected in the FTIR fingerprint, it is not known how many of the important product properties are captured by the spectra. The fingerprint can be used directly to characterise product quality, as illustrated in this work, but it is often desirable to quantify specific quality properties related to e.g. taste/smell, bioactivity, and functional properties. Protein yield is perhaps the most important parameter for the industry, and this can be calculated from the protein content in the product relative to the raw material. The FTIR fingerprints should therefore not be used alone but combined with other measurements.

To our knowledge, there currently exists no commercial solution for real-time analysis of liquids using dry-film FTIR spectroscopy. However, infrared spectroscopic technologies are being developed at a steady pace. Low-cost FTIR systems are readily available, and other alternatives are also emerging (Sieger et al., 2017). A real-time dry-film FTIR solution would require robotic sample handling and drying. Such an approach has already been proposed for a high-throughput laboratory screening system (Xiong, Shapaval, Kohler, Li, & From, 2019). Even though adjustments would be needed for an industrial system, this shows the potential of the approach. The drying procedure will affect the measurement time, but speed requirements also depend on the EPH reactor in question (i.e. batch or continuous reactor) and high speed is not always necessary. Since protein-rich droplets are known to dry quickly even at room temperatures, developments in this area are surely expected. A real-time industrial FTIR system for fingerprinting of protein hydrolysates is therefore a realistic goal for the near future.

5. Conclusion

Our results show that FTIR fingerprints contain patterns that are stable across experiments and time, and that a substantial part (77%) of the fingerprint can be related to raw material composition, enzyme, and hydrolysis time. Most of the variation is caused by differences in enzyme and hydrolysis time, but raw material composition is contributing to several of the less dominant principal components. We have also shown that the database of fingerprints can be used for evaluating industrial products without any additional knowledge about the samples. By projecting industry samples from three periods onto the map of FTIR fingerprints, we can clearly see that improvement work in the industry has led to a more stable product quality. These results lay the foundation for using FTIR spectroscopy as an industrial tool for product and process optimisation and control.

Declaration of interests

The authors declare that they have no known competing financial interests or personal relationships that could have appeared to influence the work reported in this paper.

Funding

This work was supported by the Norwegian Levy on Agricultural Products (grant number 282466, 262308 and 314111).

CRediT authorship contribution statement

Ingrid Måge: Conceptualization, Data curation, Investigation, Methodology, Formal analysis, Writing – original draft, Visualization, Project administration, Funding acquisition. **Ulrike Böcker:** Methodology, Investigation, Writing – original draft. **Sileshi Gizachew Wubshet:** Conceptualization, Investigation, Writing – original draft, Funding acquisition. **Diana Lindberg:** Conceptualization, Investigation, Writing – original draft, Funding acquisition. **Nils Kristian Afseth:** Conceptualization, Investigation, Methodology, Writing – original draft, Project administration, Funding acquisition.

Acknowledgements

We acknowledge Kenneth Aase Kristoffersen, Lene Øverby and Katinka Dankel for excellent technical assistance. We also thank Bioco and Norilia for providing raw materials and product samples, and for the partnership related to enzymatic hydrolysis.

References

Aspevik, T., Oterhals, Å., Rønning, S. B., Altintzoglou, T., Wubshet, S. G., Gildberg, A., et al. (2017, June 1). Valorization of proteins from Co- and by-products from the fish and meat industry. Topics in current chemistry. Springer verlag. https://doi.org/10.1007/s41061-017-0143-6.

Baak, M., Koopman, R., Snoek, H., & Klous, S. (2020). A new correlation coefficient between categorical, ordinal and interval variables with Pearson characteristics. *Computational Statistics and Data Analysis, 152*, 107043. https://doi.org/10.1016/j.csda.2020.107043.

Böcker, U., Wubshet, S. G., Lindberg, D., & Afseth, N. K. (2017). Fourier-transform infrared spectroscopy for characterization of protein chain reductions in enzymatic reactions. *The Analyst, 142*(15), 2812–2818. https://doi.org/10.1039/c7an00488e

FDA. (2004). Guidance for industry: PAT. Retrieved from. http://www.fda.gov/downloads/Drugs/Guidances/ucm070305.pdf.

García Arteaga, V., Apéstegui Guardia, M., Muranyi, I., Eisner, P., & Schweiggert-Weisz, U. (2020). Effect of enzymatic hydrolysis on molecular weight distribution, techno-functional properties and sensory perception of pea protein isolates. *Innovative Food Science & Emerging Technologies, 65*, 102449. https://doi.org/10.1016/j.ifset.2020.102449

Gargalo, C. L., Udugama, I., Pontius, K., Lopez, P. C., Nielsen, R. F., Hasanzadeh, A., et al. (2020). Towards smart biomanufacturing: A perspective on recent developments in industrial measurement and monitoring technologies for bio-based production processes. *Journal of Industrial Microbiology and Biotechnology*, 1–18. https://doi.org/10.1007/s10295-020-02308-1

Hassoun, A., Måge, I., Schmidt, W. F., Temiz, H. T., Li, L., Kim, H.-Y., et al. (2020). Fraud in animal origin food products: Advances in emerging spectroscopic detection methods over the past five years. *Foods, 9*(8), 1069. https://doi.org/10.3390/foods9081069

Kristoffersen, K. A. (2019). *Food and non-food applications of collagen peptides, effects of feedstock source and processing conditions*. Norwegian University of Life Sciences.

Kristoffersen, K. A., Afseth, N. K., Böcker, U., Lindberg, D., de Vogel-van den Bosch, H., Ruud, M. L., et al. (2020). Average molecular weight, degree of hydrolysis and dry-film FTIR fingerprint of milk protein hydrolysates: Intercorrelation and application in process monitoring. *Food Chemistry, 310*, 125800. https://doi.org/10.1016/J.FOODCHEM.2019.125800

Kristoffersen, K. A., Liland, K. H., Böcker, U., Wubshet, S. G., Lindberg, D., Horn, S. J., et al. (2019). FTIR-based hierarchical modeling for prediction of average molecular weights of protein hydrolysates. *Talanta, 205*(January), 120084. https://doi.org/10.1016/j.talanta.2019.06.084

Li, Z., Wang, B., Chi, C., Gong, Y., Luo, H., & Ding, G. (2013). Influence of average molecular weight on antioxidant and functional properties of cartilage collagen hydrolysates from Sphyrna lewini, Dasyatis akjei and Raja porosa. *Food Research International, 51*(1), 283–293. https://doi.org/10.1016/j.foodres.2012.12.031

Lovergne, L., Clemens, G., Untereiner, V., Lukaszweski, R. A., Sockalingum, G. D., & Baker, M. J. (2015). Investigating optimum sample preparation for infrared spectroscopic serum diagnostics. *Analytical Methods, 7*(17), 7140–7149. https://doi.org/10.1039/c5ay00502g

Nasirpour, A., Scher, J., & Desobry, S. (2006). Baby foods: Formulations and interactions (A review). *Critical Reviews in Food Science and Nutrition, 46*(8), 665–681. https://doi.org/10.1080/10408390500511896

Næs, T., Måge, I., & Segtnan, V. H. (2011). Incorporating interactions in multi-block sequential and orthogonalised partial least squares regression. *Journal of Chemometrics, 25*(11), 601–609. https://doi.org/10.1002/cem.1406

Næs, T., Tomic, O., Afseth, N. K., Segtnan, V., & Måge, I. (2013). Multi-block regression based on combinations of orthogonalisation, PLS-regression and canonical correlation analysis. *Chemometrics and Intelligent Laboratory Systems, 124*, 32–42. https://doi.org/10.1016/j.chemolab.2013.03.006

Poulsen, N. A., Eskildsen, C. E., Akkerman, M., Johansen, L. B., Hansen, M. S., Hansen, P. W., et al. (2016). Predicting hydrolysis of whey protein by mid-infrared spectroscopy. *International Dairy Journal, 61*, 44–50. https://doi.org/10.1016/J.IDAIRYJ.2016.04.002

Tang, J. E., Moore, D. R., Kujbida, G. W., Tarnopolsky, M. A., & Phillips, S. M. (2009). Ingestion of whey hydrolysate, casein, or soy protein isolate: Effects on mixed muscle protein synthesis at rest and following resistance exercise in young men. *Journal of Applied Physiology, 107*(3), 987–992. https://doi.org/10.1152/japplphysiol.00076.2009

Valand, R., Tanna, S., Lawson, G., & Bengtström, L. (2020). A review of Fourier Transform Infrared (FTIR) spectroscopy used in food adulteration and authenticity investigations. *Food Additives & Contaminants Part A Chemistry, Analysis, Control, Exposure and Risk Assessment, 37*(1), 19–38. https://doi.org/10.1080/19440049.2019.1675909

Vidal-Puig, S., Vitale, R., & Ferrer, A. (2019). Data-driven supervised fault diagnosis methods based on latent variable models: a comparative study. Chemometrics and Intelligent Laboratory Systems, 187(January), 41–52. https://doi.org/10.1016/j.chemolab.2019.02.006.

Wang, Q., Hulzebosch, A., & Bovenhuis, H. (2016). Genetic and environmental variation in bovine milk infrared spectra. *Journal of Dairy Science, 99*(8), 6793–6803. https://doi.org/10.3168/jds.2015-10488

Wold, S., & Sjöström, M. (1977). *Simca: A method for analyzing chemical data in terms of similarity and analogy*. https://doi.org/10.1021/bk-1977-0052.ch012

Wubshet, S. G., Lindberg, D., Veiseth-Kent, E., Kristoffersen, K. A., Böcker, U., Washburn, K. E., & Afseth, N. K. (2019). Bioanalytical Aspects in Enzymatic Protein Hydrolysis of By-Products. In *Proteins: Sustainable Source, Processing and Applications* (pp. 225–258). Elsevier. https://doi.org/10.1016/b978-0-12-816695-6.00008-8.

Wubshet, S. G., Måge, I., Böcker, U., Lindberg, D., Knutsen, S. H., Rieder, A., et al. (2017). FTIR as a rapid tool for monitoring molecular weight distribution during enzymatic protein hydrolysis of food processing by-products. *Anal. Methods, 9*(29), 4247–4254. https://doi.org/10.1039/C7AY00865A

Wubshet, S. G., Wold, J. P., Afseth, N. K., Böcker, U., Lindberg, D., Ihunegbo, F. N., et al. (2018). Feed-forward prediction of product qualities in enzymatic protein hydrolysis of poultry by-products: A spectroscopic approach. *Food and bioprocess technology*. https://doi.org/10.1007/s11947-018-2161-y

Xiong, Y., Shapaval, V., Kohler, A., Li, J., & From, P. J. (2019). A Fully Automated Robot for the Preparation of Fungal Samples for FTIR Spectroscopy Using Deep Learning. *IEEE Access, 7*, 132763–132774. https://doi.org/10.1109/ACCESS.2019.2941704.

Zaalberg, R. M., Shetty, N., Janss, L., & Buitenhuis, A. J. (2019). Genetic analysis of Fourier transform infrared milk spectra in Danish Holstein and Danish Jersey. *Journal of Dairy Science, 102*(1), 503–510. https://doi.org/10.3168/jds.2018-14464

Zhang, X., Thiéfin, G., Gobinet, C., Untereiner, V., Taleb, I., Bernard-Chabert, B., et al. (2013). Profiling serologic biomarkers in cirrhotic patients via high-throughput Fourier transform infrared spectroscopy: Toward a new diagnostic tool of hepatocellular carcinoma. *Translational Research, 162*(5), 279–286. https://doi.org/10.1016/j.trsl.2013.07.007